PHYSICAL REVIEW B

CONDENSED MATTER AND MATERIALS PHYSICS

THIRD SERIES, VOLUME 57, NUMBER 11 **15 MARCH 1998-I**

BRIEF REPORTS

Brief Reports are accounts of completed research which, while meeting the usual **Physical Review B** *standards of scientific quality, do not warrant regular articles. A Brief Report may be no longer than four printed pages and must be accompanied by an abstract. The same publication schedule as for regular articles is followed, and page proofs are sent to authors.*

First-principles study of Zn-Sb thermoelectrics

Seong-Gon Kim
UES, Inc. and Code 6691, Complex Systems Theory Branch, Naval Research Laboratory, Washington, D.C. 20375-5000

I. I. Mazin
Computational Science Institute, George Mason University, Fairfax, Virginia 22030
and Code 6691, Complex Systems Theory Branch, Naval Research Laboratory, Washington, D.C. 20375-5000

D. J. Singh
Code 6691, Complex Systems Theory Branch, Naval Research Laboratory, Washington, D.C. 20375-5000

(Received 23 September 1997)

We report local-density-approximation calculations of the electronic structure and thermoelectric properties of β-Zn_4Sb_3. The material is a low carrier density metal with a complex Fermi-surface topology and a nontrivial dependence of the Hall concentration on the band filling. The band structure is rather covalent, consistent with experimental observations of good carrier mobility. At a band filling corresponding to the experimental Hall number, the calculated thermopower and temperature dependence are in good agreement with experiment. The high Seebeck coefficient in a metallic material is remarkable, and arises in part from the strong energy dependence of the Fermi surface topology near the experimental band filling. An improved thermoelectric performance is predicted for lower doping levels, i.e., higher Zn concentrations. [S0163-1829(98)02011-6]

There has been a revival of activity in the search for improved thermoelectrics, with an emphasis on nontraditional materials systems.[1] The dimensionless figure of merit is $ZT = \sigma S^2 T/\kappa = S^2/L$, where T is the temperature, σ is the electrical conductivity, S is the Seebeck coefficient (thermopower), and κ is the thermal conductivity, which contains both electronic and lattice contributions, $\kappa = \kappa_{el} + \kappa_{lat}$. The Lorentz number $L = \kappa/\sigma T$ is ordinarily limited from below by its electronic value $\kappa_{el}/\sigma T$, given by the Wiedemann-Franz value $L = (\pi^2/3)(k_B/e)$.[2] Current thermoelectric materials have $ZT \approx 1$. With the Wiedemann-Franz value for L, $ZT > 1$ requires $S > 160$ μV/K. Such values may occur in doped semiconductors, so much thermoelectric research has focused on covalent semiconducting compounds and alloys, composed of fourth- and fifth-row elements, with a view to finding low thermal conductivity materials that have reasonable carrier mobilities and high band masses, e.g., Bi_2Te_3, Si-Ge, and PbTe compounds. Despite efforts spanning three decades, little progress in increasing ZT has been achieved until recently, and in particular Bi_2Te_3/Sb_2Te_3 has remained as the material of choice for room-temperature applications.

In the last two years, however, three materials with $ZT \gtrsim 1$ have been reported,[2–4] and these do not clearly fall into the same class. One of these materials, β-Zn_4Sb_3, with a reported $ZT \approx 1.3$, has a large region of linear temperature dependence of the resistivity (Fig. 1), suggestive of a metallic rather than semiconducting material. But, unlike normal metals, this is accompanied by high thermopowers.

Here we present first-principles calculations, within the local-density approximation (LDA), after our previous calculations for binary and filled skutterudites.[5–8] The goal is to understand the remarkable thermoelectric properties of β-Zn_4Sb_3 by analyzing transport properties using the band structure.

The computations were performed self-consistently

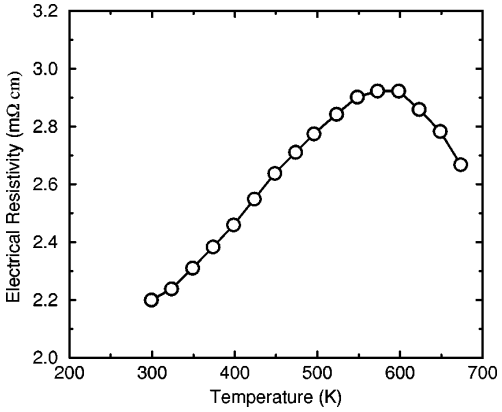

FIG. 1. Experimental resistivity of β-Zn_4Sb_3, plotted with a linear temperature scale using data of Ref. 2.

within the LDA using the general potential linearized augmented plane-wave (LAPW) method.[9,10] This method is well suited to materials with open crystal structures and low site symmetries like β-Zn_4Sb_3. Special care has been taken to obtain a well converged basis set of approximately 2100 functions with LAPW sphere radii of 2.5 a.u. for both Zn and Sb atoms. Zone averages for self-consistency used ten special **k** points in the irreducible wedge; 781 inequivalent **k** points were used for transport calculations. This relatively large number of **k** points was needed to obtain accurate Fermi velocities, and, especially, Hall coefficients. Local orbitals[11] were used to relax linearization errors. The LDA (Ref. 12) calculations were based on the experimental crystal structure of β-Zn_4Sb_3 (Ref. 13) shown in Fig. 2; however, the site reported to have approximately 11% of Zn and 89% of Sb (light gray spheres in Fig. 2) was taken to be a pure Sb site. This yields a formula Zn_6Sb_5 with 22 atoms per rhombohedral unit cell. The mixed occupancy was then accounted for in a rigid-band way, as discussed below. Of the five Sb atoms three occupy the mixed site ($Sb^{(m)}$), and two are on a

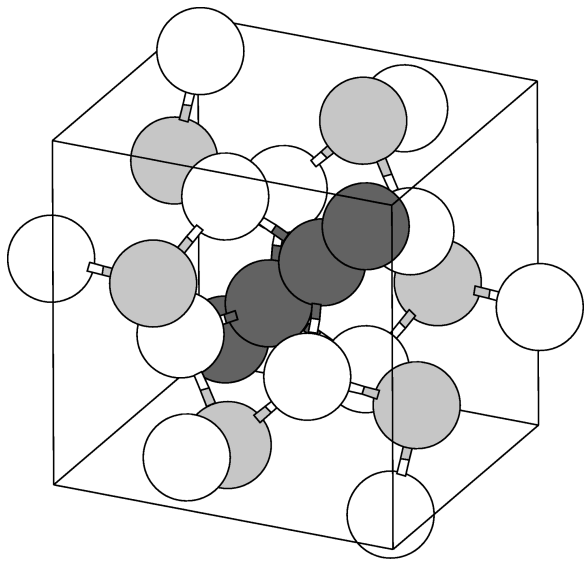

FIG. 2. Crystal structure of β-Zn_4Sb_3. White and dark gray spheres denote the 12 Zn and four Sb atoms on pure sites in the 22-atom rhombohedral unit cell. Six light gray spheres are occupied by 89% of Sb and 11% of Zn atoms.

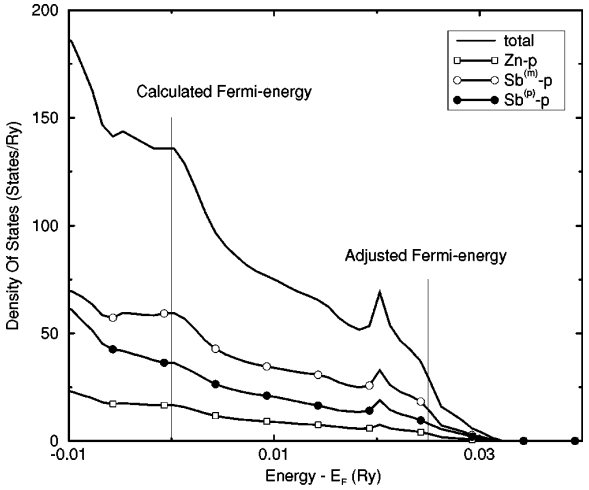

FIG. 3. Total and partial DOS's of β-Zn_4Sb_3. The DOS is per cell, and the partial DOS's are per atom magnified by a factor 10 for clarity. Note the highly covalent character. Calculations are for the stoichiometric composition (E_F at lower vertical line). The actual E_F is at the upper marker.

pure Sb site ($Sb^{(p)}$). Two $Sb^{(p)}$ atoms form $Sb_2^{(p)}$ dimers parallel to the rhombohedral axis with bond length 2.82 Å: just twice the Sb covalent radius. Covalent $Sb^{(p)}$-$Sb^{(p)}$ bonding is confirmed by the band structure calculations. Each $Sb^{(p)}$ forms three additional bonds with Zn, thus being essentially fourfold coordinated. These are also largely covalent; cf. the partial density of states (DOS) shown in Fig. 3.

Both Zn and $Sb^{(m)}$ occur in high coordinated positions; Zn forms one bond with $Sb^{(p)}$, one bond with another Zn, and three bonds with $Sb^{(m)}$, while $Sb^{(m)}$ forms all six bonds with Zn. The similar coordination of Zn and $Sb^{(m)}$ favors Zn substituting on $Sb^{(m)}$ over $Sb^{(p)}$, as observed. Substituting one $Sb^{(m)}$ by a Zn eliminates six Zn-Sb bonds and creates six Zn-Zn bonds. In general, this is not energetically favorable, and one could expect stoichiometric Zn_6Sb_5 rather than Zn-rich $Zn_{6.33}Sb_{4.77}$, observed experimentally. However, in the stoichiometric compound, as discussed below, the bonding states of Sb are not yet completely filled, and doping electrons into the system produces additional bonding. The balance between the two effects may account for the partial substitution; however, the very narrow range of compositions for which samples exist remains unexplained.

As mentioned, our calculations were done for the stoichiometric structure. The Fermi level E_F lies $\approx$0.4 eV below the top of the valence band, which is separated by a sizable gap (also $\approx$0.4 eV) from the conduction bands. The deviation from stoichiometry is taken into account by a rigid-band approach where the electronic structure is fixed as calculated and the position of E_F is shifted. This is expected to be valid in a highly covalent, broad band system as we find, and is supported *a posteriori* by comparison with experiment. We calculated the transport properties as functions of E_F, and used the experimental Hall conductivity to fix E_F corresponding to actual samples.

The transport properties were determined using the standard kinetic theory as given by Ziman and others.[14,15] For the electrical conductivity, the Bloch-Boltzmann kinetic equa-

tion in lowest order along the x direction is (similarly for the other Cartesian directions)

$$\sigma_x(T)=e^2\int d\epsilon\ N(\epsilon)v_x^2(\epsilon)\tau(\epsilon,T)\left[-\frac{\partial f(\epsilon)}{\partial\epsilon}\right]. \quad (1)$$

$N(\epsilon)$ is the DOS at energy ϵ per unit volume, τ is the scattering rate for electrons, and $v_x^2(\epsilon)$ is defined by

$$N(\epsilon)v_x^2(\epsilon)=\frac{2}{(2\pi)^3}\int v_x^2\frac{dS_\epsilon}{v_\epsilon}, \quad (2)$$

$$N(\epsilon)=\frac{2}{(2\pi)^3}\int\frac{dS_\epsilon}{v_\epsilon}. \quad (3)$$

The integrations are carried out over the isoenergy surface, dS_ϵ, defined by $\epsilon_{\mathbf{k}}=\epsilon$. For $\epsilon_{\mathbf{k}}=E_F$, the integral is over the Fermi surface and v_ϵ is the Fermi velocity. Then it is related to the square of the plasma frequency $\omega_{p_x}^2=4\pi e^2N(E_F)v_x^2(E_F)$, which is proportional to the optical carrier concentration $(n/m)_{\text{eff}}=N(E_F)v_x^2(E_F)$. We note that in general this does not have a simple relationship to the Hall concentration or the electron count (i.e., the doping level); the Hall concentration is a measure of the average curvature of the Fermi surface, while the doping level is determined by the volume enclosed by the Fermi surface.

For isotropic scattering, which is often a reasonable approximation, the relaxation time does not enter the expression for the Hall concentration, yielding[15,16]

$$n_H=-\sigma^2/e\sigma_H \quad (4)$$

with

$$\sigma_H=\frac{e^3}{12}\int d\epsilon N(\epsilon)\mathbf{v}(\epsilon)\cdot[\mathrm{Tr}(\mathbf{M}^{-1})-\mathbf{M}^{-1}]\cdot\mathbf{v}(\epsilon)\tau^2(\epsilon,T)\times\left[-\frac{\partial f(\epsilon)}{\partial\epsilon}\right], \quad (5)$$

where for simplicity we have given the expression for cubic symmetry. $\mathbf{M}$ is the $\mathbf{k}$-dependent effective-mass tensor,

$$\mathbf{M}_{\alpha\beta}^{-1}\equiv\hbar^{-1}\frac{\partial v_\alpha}{\partial k_\beta}\equiv\hbar^{-2}\frac{\partial^2\epsilon_k}{\partial k_\alpha\partial k_\beta}. \quad (6)$$

If the Fermi surface topology does not vary strongly on the scale of k_BT, the derivatives of the Fermi distribution in the above expressions may be replaced by the $T=0$ limit, thereby suppressing the energy integrals. This approximation was used in the calculations of the Hall concentrations in this paper. However, in the expression for the Seebeck coefficient S, one has to include the energy dependence explicitly at temperatures several times smaller than the characteristic electronic energy scale. Thus we have used the full expression

$$S(T)=\frac{1}{eT\sigma(T)}\int d\epsilon\ \epsilon\sigma(\epsilon,T)\left[-\frac{\partial f(\epsilon)}{\partial\epsilon}\right], \quad (7)$$

where

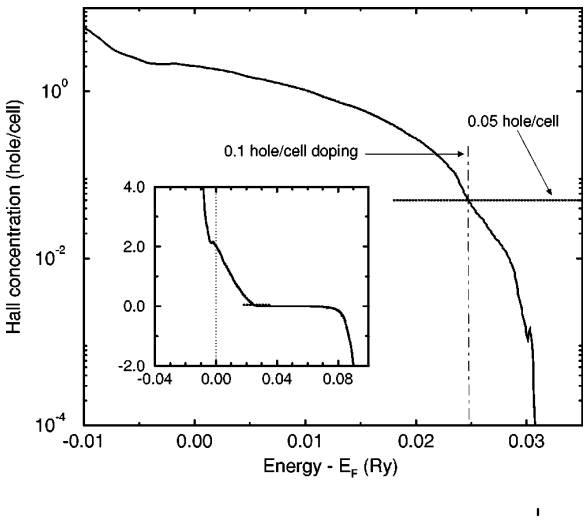

FIG. 4. Hall concentration vs E_F relative to the stoichiometric solid (solid line) on a linear-log plot. The inset shows the same quantity over a wider range, including both sides of the gap. The dotted horizontal line is the experimental value, and the dot-dashed line is the Fermi-level shift to match the measured Hall concentration.

$$\sigma(\epsilon,T)=e^2N(\epsilon)v_x^2(\epsilon)\tau(\epsilon,T) \quad (8)$$

is the conductivity corresponding to a E_F positioned at ϵ. The expression for $\sigma(\epsilon,T)$ in Eq. (8) contains two energy-dependent factors; a factor related to the square of the plasma frequency, $\omega_{px}^2=4\pi e^2Nv_x^2$, and the relaxation time τ. Ordinarily, the first term is the most energy dependent, but there are exceptions,[17] e.g., Pd metal, where E_F occurs near a very sharp feature in $N(\epsilon)$, and Kondo systems where there is resonant scattering.[15] Since β-Zn_4Sb_3 does not show any indication of such behavior, we approximated the energy dependence of σ using only the Nv_x^2 term.

β-Zn_4Sb_3 has a small Hall number, and is characterized either as a low carrier density metal or a heavily doped semiconductor. The former terminology is probably more appropriate, because the resistivity[2] increases linearly with T over a wide range of at least 300 K$<T<$550 K (see Fig. 1). The Hall number $n_H=9\times10^{19}$ cm$^{-3}=0.05$ holes/cell for the reported high ZT sample, although small for a metal, may be too large to allow analysis of the transport in terms of usual semiconductor formulas. The Hall concentration calculated according to Eq. (5) is plotted in Fig. 4 as a function of the Fermi-level shift from its position in the stoichiometric compound. Note that n_H is not simply related to the band filling; the experimental Hall number of 0.05 holes/cell corresponds to a filling of 0.1 holes/cell, roughly twice n_H. Here $\omega_p=1-1.2$ eV (depending on polarization), i.e., $(n/m)_{\text{eff}}\approx0.5(m_0/m)$ holes/cell, with m_0 being the bare electron mass. The main sheet of the Fermi surface (see Fig. 5), near the top of the valence band in the range relevant to high ZT samples, is more toroidal than ellipsoidal. Thus, even at this low carrier density, the Fermi surface has a complicated shape with electronlike and holelike contributions. This explains why the Hall concentration is so different from the doping level, and also suggests that the Fermi velocity and

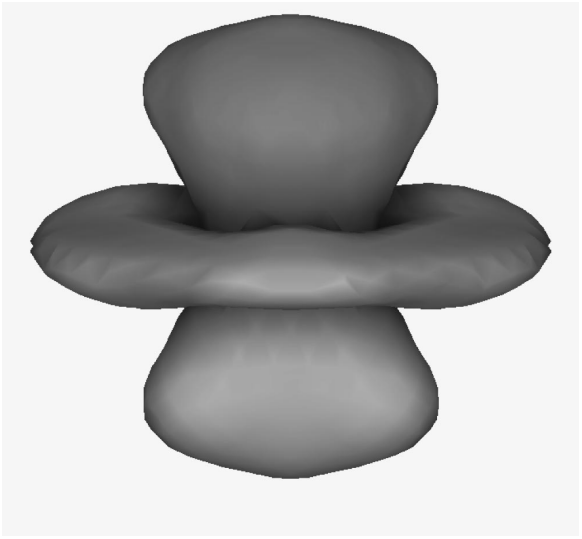

FIG. 5. Main Fermi surface of β-Zn_4Sb_3 at the experimental band filling.

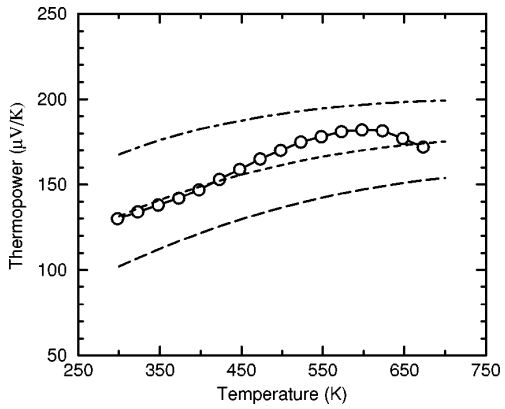

FIG. 6. Calculated (short dashes) and experimental (solid line with open circle) thermopower for β-Zn_4Sb_3 with a 0.05 hole/cell Hall concentration (0.10 hole/cell doping). $S(T)$ for Hall concentrations 0.12 and 0.02 hole/cell (0.15 and 0.04 hole/cell doping level) are given by the curves above (dot-dashed) and below (long dashed) for comparison.

conductivity may depend on the Fermi-level position in a strong and unusual way. This is the case, and it is partially responsible for the high thermopower.

Indeed, using Eq. (7), we find a rather high Seebeck coefficient (Fig. 6). Naturally, S depends strongly on E_F. Comparison with the experiment shows very good agreement for the hole count of 0.1 hole/cell. This is exactly the hole count that we deduced from the measured Hall number of 0.05 holes/cell, demonstrating the consistency of our approach.

As mentioned, the experimental resistivity up to approximately 550 K shows metallic behavior with $d\rho/dT \approx 3.1$ $\mu\Omega$ cm/K and residual resistivity $\rho_0 \approx 1.8$ mΩ cm. From these data and the calculated plasma frequency, one can estimate the transport electron-phonon coupling constant λ_{tr} and the scattering rate γ due to static defects, to obtain $\lambda_{tr} \approx 1$ and $\gamma \approx 0.2$ eV. Both numbers are relatively large, but may be overestimates, as they are not based on single-crystal data. In any case, the experimental data indicate that at high temperature κ is mainly κ_{el} in the best reported sample. This implies that variations in the doping level that increase S will also increase ZT. Our calculations show, not unexpectedly, that raising the Fermi energy corresponding to lower carrier concentration leads to higher values of S, particularly at intermediate temperatures ranging from room temperature to the maximum temperature. This corresponds to higher Zn concentrations on the mixed site.

We characterize this material as a metal with a complex, energy-dependent Fermi surface. This helps provide large thermopower for relatively high carrier concentration. The β-Zn_4Sb_3 system is apparently not optimized for thermoelectric application, and further increases in ZT are expected if the doping level is reduced. One important issue revolves around the question of why it is so difficult to make samples with varying Zn concentrations on the mixed site, since higher Zn concentration would lead to higher ZT. We speculate that the reason for this has to do with competition from other phases during the high-temperature synthesis. It would be very interesting to attempt growth by other nonequilibrium processes such as pulsed laser deposition.

The authors are grateful for helpful discussions with T. Caillat and J. P. Fleurial. Computations were performed using DoD HPCMO facilities at NAVO and ASC. This work was supported by DARPA. Work at NRL was supported by the ONR.

[1] G. Mahan, B. Sales, and J. Sharp, Phys. Today **50** (3), 42 (1997).

[2] T. Caillat, J. P. Fleurial, and A. Borshchevsky, in *Proceedings ICT'96*, edited by T. Caillat, A. Borshchevsky, and J. P. Fleurial (IEEE, Piscataway, NJ, 1996), p. 151.

[3] B. C. Sales, D. Mandrus, and R. K. Williams, Science **272**, 1325 (1996).

[4] J. P. Fleurial, A. Borshchevsky, T. Caillat, and G. P. Meisner, in *Proceedings ICT'96* (Ref. 2), p. 91.

[5] D. J. Singh and I. I. Mazin, Phys. Rev. B **56**, R1650 (1994).

[6] L. Nordstrom and D. J. Singh, Phys. Rev. B **53**, 1103 (1996).

[7] D. J. Singh and W. E. Pickett, Phys. Rev. B **50**, 11235 (1994).

[8] J. L. Feldman and D. J. Singh, Phys. Rev. B **53**, 6273 (1996); **54**, 712 (1996).

[9] O. K. Anderson, Phys. Rev. B **12**, 3060 (1975).

[10] D. J. Singh, *Planewaves, Pseudopotential and the LAPW Method* (Kluwer, Boston, 1994).

[11] D. J. Singh, Phys. Rev. B **43**, 6388 (1991).

[12] L. Hedin and B. I. Lundqvist, J. Phys. C **4**, 2064 (1971).

[13] P. Villars and L. D. Calvert, *Pearson's Handbook of Crystallographic Data for Intermetallic Phases*, 2nd ed. (ASM International, Materials Park, OH, 1991), p. 5206.

[14] J. M. Ziman, *Principles of the Theory of Solids* (Cambridge University Press, Cambridge, 1972).
[15] C. M. Hurd, *The Hall Effect in Metallic and Alloys* (Plenum, New York, 1972).
[16] W. W. Schulz, P. B. Allen, and N. Trivedi, Phys. Rev. B **45**, 10 886 (1992).
[17] A. E. Karakosov, I. I. Mazin, and Y. A. Uspenski, Sov. Phys. Dokl. **277**, 848 (1984).